Liquid Crystals
Publication details, including instructions for authors and subscription information:
http://www.informaworld.com/smpp/title~content=t713926090

Heat capacities and phase transitions of the antiferroelectric liquid crystals MHPOBC and MHPOCBC

S. Asahina; M. Sorai; A. Fukuda; H. Takezoe; Y. Suzuki; I. Kawamura; K. Furukawa; K. Terashima

Online publication date: 29 June 2010

To cite this Article Asahina, S. , Sorai, M. , Fukuda, A. , Takezoe, H. , Suzuki, Y. , Kawamura, I. , Furukawa, K. and Terashima, K.(1997) 'Heat capacities and phase transitions of the antiferroelectric liquid crystals MHPOBC and MHPOCBC', Liquid Crystals, 23: 3, 339 — 348
To link to this Article: DOI: 10.1080/026782997208262
URL: http://dx.doi.org/10.1080/026782997208262

LIQUID CRYSTALS, 1997, VOL. 23, NO. 3, 339–348

Heat capacities and phase transitions of the antiferroelectric liquid crystals MHPOBC and MHPOCBC†

by S. ASAHINA and M. SORAI*
Microcalorimetry Research Center, Faculty of Science, Osaka University, Toyonaka, Osaka 560, Japan

A. FUKUDA and H. TAKEZOE
Department of Organic and Polymeric Materials, Tokyo Institute of Technology, O-okayama, Meguro-ku, Tokyo 152, Japan

K. FURUKAWA
Chisso Co., Kamariya 2, Kanazawa-ku, Yokohama, Kanagawa 236, Japan

K. TERASHIMA
Chisso Petrochemical Co., Research Center, Goikaigan 5-1, Ichihara, Chiba 290, Japan

Y. SUZUKI and I. KAWAMURA
Showa Shell Sekiyu K. K., Central Research and Development Laboratory, Shimokawairi 123-1, Atsugi, Kanagawa 243-02, Japan

(*Received 25 November 1996; in final form 7 April 1997; accepted 8 April 1997*)

Heat capacities of the antiferroelectric liquid crystals 4-(1-methylheptyloxycarbonyl)phenyl-4′-octyloxybiphenyl-4-carboxylate (MHPOBC) and 4-(1-methylheptyloxycarbonyl)phenyl-4′-octylcarboxybiphenyl-4-carboxylate (MHPOCBC), have been measured with an adiabatic calorimeter between 350 and 460 K. MHPOBC showed three smectic subphases (ferrielectric C_γ^*, ferroelectric C* and a fancy phase C_α^*) between antiferroelectric smectic C_A^* and paraelectric smectic A, while MHPOCBC exhibited only one subphase (smectic C_α^*). These phases are clearly discriminated by the existence of phase transitions. The enthalpies and entropies gained at the respective phase transitions were very small. A much larger phase transition from smectic A to isotropic liquid was also observed in both compounds.

1. Introduction

Since the discovery of antiferroelectric liquid crystals, various studies have been performed from the standpoints of not only fundamental interest in aggregated states of molecules but also of potential applicabilities to electro-optical devices. In particular, 4-(1-methylheptyloxycarbonyl)phenyl-4′-octyloxybiphenyl-4-carboxylate (MHPOBC) has drawn marked attention owing to its interesting physical features. This mesogen shows tristable switching characteristics between the ferroelectric smectic C* phase (SmC*) and the antiferroelectric smectic C_A^* phase (SmC_A^*) under application of an electric field. Even in the absence of an electric field, MHPOBC also exhibits the ferro- and antiferroelectric liquid crystalline states as the polymorph of SmC* when the specimen temperature is varied. To clarify the characteristic properties of MHPOBC, dielectric measurements [1–3], electro-optic measurements [1], conoscopic observation [1, 4], circular dichroism measurements [5], texture observation [6, 7], X-ray diffraction analysis [1, 8, 9], infrared spectroscopy [10, 11] and Raman scattering measurements [9] have so far been carried out.

For the calorimetric studies of MHPOBC, differential scanning calorimetry (DSC), alternating current (a.c.) calorimetry, and measurements of relaxation have

†Contribution No. 121 from the Microcalorimetry Research Center.

*Author for correspondence.

0267–8292/97 $12·00

already been performed [1, 4, 7, 9, 12–15]. The DSC study indicated that MHPOBC with high optical purity exhibits the smectic C_γ^* (SmC_γ^*) phase between the antiferroelectric SmC_A^* and ferroelectric SmC* phases, and the smectic C_α^* (SmC_α^*) phase between the ferroelectric SmC* and paraelectric smectic A (SmA) phases, while its racemate brings about neither the SmC_α^* nor SmC_γ^* phase. a.c. calorimetric measurements sensed only the heat capacity anomaly arising from the second order phase transition between the SmC_α^* and SmA phases. This fact suggests that the phase transitions occurring between the smectic C* subphases in MHPOBC would be first order and this is confirmed by relaxation calorimetry [12].

The purpose of the present study is to measure the heat capacities of this interesting antiferroelectric liquid crystal MHPOBC with an adiabatic calorimeter and to elucidate its thermodynamic properties. Together with MHPOBC, we also measured the heat capacities of another antiferroelectric liquid crystal, 4-(1-methylheptyloxycarbonyl)phenyl-4′-octylcarboxybiphenyl-4-carboxylate (MHPOCBC). As shown in figure 1, MHPOCBC has the same molecular structure as MHPOBC except for the carboxyl group located between the octyl and the biphenyl groups [16]. Although the molecular structures bear close resemblance to each other, their phase sequences are different [12, 17]. On the basis of the calorimetric measurements we shall discuss this problem.

2. Experimental

The compounds of interest, MHPOBC and MHPOCBC with high purity, were prepared by Terashima and Furukawa and by Suzuki and Kawamura, respectively. Prior to the adiabatic heat capacity measurements, preliminary thermal investigations were made by using a differential scanning calorimeter (Perkin–Elmer, DSC-7) for both samples.

Heat capacities were measured with an adiabatic calorimeter in the range 350 to 460 K [18]. The calorimeter cell consisted of a sample container ($\sim 10\,cm^3$ in volume) made of gold-plated beryllium copper, a thermometer and a heater. The temperature of the calorimeter cell was measured with a platinum resistance thermometer (Minco Co., Ltd.), whose temperature scale was calibrated on the basis of the IPTS-68. In order to get as much sample into the cell as possible, the calorimeter cell was loaded with a repeated load–melt–freeze cycle of sample addition under a helium gas atmosphere. The cell was filled to ~ 60 per cent of its total volume. The amount of sample used was 0·011091 mol MHPOBC (equivalent to 6·1974 g after a buoyancy correction using the sample density of $1{\cdot}10\,g\,cm^{-3}$) and 0·0088916 mol MHPOCBC (equivalent to 5·2173 g). A small amount of helium gas (300 Torr) was sealed in the cell to aid the heat transfer.

MHPOBC

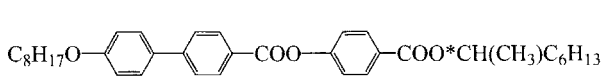

MHPOCBC

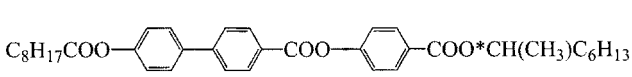

Figure 1. Molecular structures of MHPOBC and MHPOCBC. An asterisk indicates the chiral centre.

3. Results and discussion

Calorimetry was carried out in five series for MHPOBC and six series for MHPOCBC. The results were evaluated in terms of molar heat capacities at constant pressure, C_p. Strictly speaking, in both cases, correction for the vaporization of the sample into the free space of the calorimeter cell should be made for the heat capacities of the liquid state. However, since the vapour pressure seems to be very small and the free space of the cell is also small, we neglected this correction.

For both compounds, the heat capacities were measured only in their liquid crystalline and isotropic liquid phases for the following reasons: First, the preliminary DSC experiment suggested that it takes a very long time to realize the most stable crystalline phase existing just below their melting points by annealing the specimen once melted. Secondly, there was the fear of decomposition of the compounds during such a long annealing period at high temperatures.

3.1. *MHPOBC*

The molar heat capacities of MHPOBC were measured in the range of 350 to 460 K. The results are listed in table 1 and plotted in figure 2. The melting temperature of crystalline MHPOBC observed by our preliminary DSC measurement after annealing for 19 h at 355·4 K was 356·5 K. This is comparable to the value (356·9 K) obtained by the relaxation calorimetry [12]. The lowest-temperature mesophase that MHPOBC shows just above the melting point is the antiferroelectric SmC_A^* phase. In a narrow temperature region from 392 to 397 K, three first order and one second order phase transitions successively occur between the antiferroelectric SmC_A^* and paraelectric SmA phases. This feature is shown in figure 3 in enlarged scale. Three subphases are clearly discriminated by these phase transitions. They are the SmC_γ^*, SmC* and SmC_α^* phases in order of increasing temperature. According to the

Table 1. Molar heat capacities of MHPOBC.

T/K	C_p/J K^{-1} mol^{-1}	T/K	C_p/J K^{-1} mol^{-1}	T/K	C_p/J K^{-1} mol^{-1}
			Series 1		
361·414	1121·6	371·581	1142·4	382·247	1171·1
362·344	1123·9	373·113	1145·8	383·759	1175·7
363·889	1126·3	374·643	1148·8	385·267	1181·5
365·432	1129·4	376·169	1154·0	386·771	1186·8
366·973	1132·7	377·694	1157·3	388·272	1193·2
368·510	1136·0	379·215	1160·9	389·766	1200·7
370·047	1138·4	380·732	1166·9		
			Series 2		
353·819	1114·9	360·026	1121·6	366·206	1132·0
355·372	1116·6	361·574	1124·3	367·746	1135·1
356·925	1118·2	363·120	1125·8	369·283	1137·7
358·477	1119·3	364·664	1128·8	370·818	1141·4
			Series 3		
385·445	1179·6	392·494	1217·8	395·620	1263·2
385·752	1182·3	392·744	1240·3	395·867	1265·5
386·215	1184·1	392·943	1244·5	396·187	1283·6
386·831	1186·4	393·143	1236·0	396·531	1288·8
387·447	1188·9	393·341	1240·4	396·879	1227·3
388·062	1191·1	393·541	1235·5	397·231	1221·2
388·676	1195·8	393·738	1289·6	397·608	1221·9
389·290	1197·1	393·934	1257·7	398·012	1219·4
389·903	1201·9	394·133	1233·9	398·417	1219·7
390·515	1205·3	394·383	1237·4	398·923	1219·2
391·126	1208·6	394·683	1242·8	399·530	1219·9
391·583	1209·6	394·982	1251·2	400·138	1219·6
391·887	1213·2	395·229	1289·3	400·746	1221·0
392·190	1215·9	395·424	1288·4		
			Series 4		
390·197	1203·3	393·641	1280·1	396·123	1276·1
390·811	1205·7	393·838	1265·3	396·319	1296·1
391·346	1208·5	394·037	1236·9	396·514	1305·0
391·728	1211·1	394·238	1234·1	396·763	1231·7
392·033	1213·9	394·438	1236·9	397·141	1223·7
392·337	1216·0	394·688	1242·3	397·673	1218·9
392·615	1229·5	394·988	1249·9	398·282	1218·9
392·840	1250·6	395·285	1299·3	398·891	1218·5
393·040	1237·7	395·531	1258·0	399·499	1219·4
393·241	1235·0	395·728	1263·9	400·107	1219·7
393·442	1229·0	395·936	1267·9	400·715	1221·9
			Series 5		
398·985	1219·9	421·719	75271	438·814	1284·5
400·471	1221·7	421·733	78638	440·252	1283·4
401·955	1222·8	421·748	71357	441·691	1283·1
403·437	1226·4	421·767	46178	443·132	1280·4
404·916	1229·9	421·887	3833·7	444·575	1279·4
406·392	1233·8	422·203	1383·0	446·016	1278·6
407·866	1238·4	423·117	1348·7	447·458	1277·5
409·337	1242·2	424·527	1335·8	448·900	1276·8
410·805	1247·7	425·941	1324·4	450·341	1277·6
412·270	1251·1	427·360	1317·9	451·782	1276·7
413·730	1257·7	428·783	1310·2	453·224	1275·8
415·187	1265·2	430·210	1305·5	454·666	1276·3
416·638	1274·3	431·632	1299·8	456·106	1277·3
418·085	1282·4	433·065	1296·2	457·546	1277·2
419·526	1295·0	434·500	1292·4	458·986	1275·0
420·955	1323·7	435·937	1289·3	460·424	1276·3
421·688	21409	437·374	1287·6		

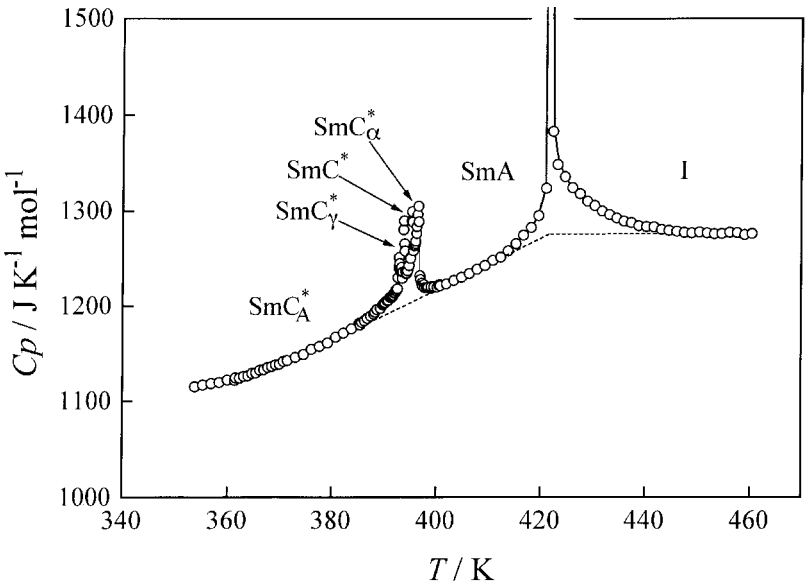

Figure 2. Molar heat capacity of MHPOBC in the range from 350 to 460 K. Broken lines indicate the normal heat capacities.

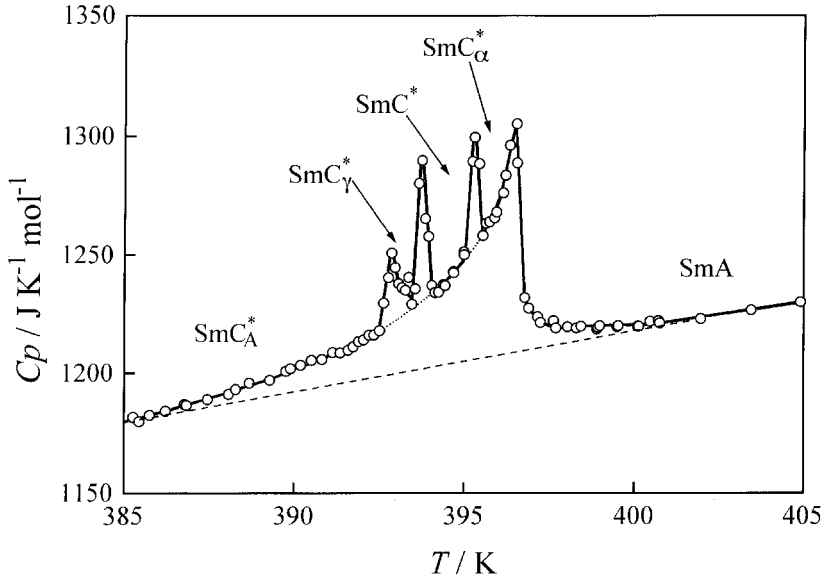

Figure 3. Molar heat capacity of MHPOBC in the phase transition region from the SmC$^*_A$ phase to the SmA phase. The broken line denotes the normal heat capacity, while the dotted curves indicate the borderlines to separate the first order components inherent in the phase transitions occurring between the SmC* subphases.

circular dichroism (CD) measurements, the SmC$^*_\gamma$ phase is ferrielectric and is composed of ferroelectric and antiferroelectric structures in the ratio of 1:2 [5]. The SmC* phase has an ordinary ferroelectric structure in which the electric dipole moments of the molecules are orientated in the same direction. The SmC$^*_\alpha$ phase is a fancy phase where the intra- and inter-layer correlations of molecular tilting are greatly reduced [1] and the helical pitch also becomes smaller than that in the SmC* phase [19]. Hiraoka *et al.* [20], have proposed 'the Devil's staircase' structure [21, 22] for the SmC$^*_\alpha$ phase, where the period concerning the arrangement of the molecular dipole moments, with respect to the smectic layers, would be infinitely changeable. Above the second order transition, MHPOBC exhibits the paraelectric SmA phase, which is transformed to the isotropic liquid at 421·73 K.

In order to determine the excess heat capacities due to the phase transitions, we estimated the so-called 'normal heat-capacity' curves for the SmC* subphases, SmA and isotropic liquid. In the case of the SmC* subphases, the normal heat-capacity curve was approxi-

mated by a straight line determination by the least square fitting to five C_p points in the 373–380 K range in the SmC_A^* phase and four C_p data in the 404–410 K range in the SmA phase (see figure 3).

Moreover, to separate the first order components inherent in the phase transitions occurring between the SmC* subphases, a borderline which might correspond to the low temperature tail of the second order phase transition between the SmC_A^* and SmA phases was assumed. To this end, a fifth order polynomial of temperature was applied to seven C_p points in the SmC_A^* phase, two C_p data in the SmC* phase and two C_p data in the SmC_α^* phase. The borderline thus obtained is shown in figure 3 as the dotted curve.

For the SmA phase and isotropic liquid, the normal heat capacity was approximated by two straight lines determinations by the least square fitting method for the heat capacity data in the vicinity of the clearing point. The straight line for the SmA phase was determined by the use of four C_p data in the 404–410 K range, while the baseline in the isotropic liquid was determined by the use of six C_p data in the 453–461 K range. As shown in figure 2 by dashed lines, these two straight lines were connected vertically at the clearing temperature.

3.2. *MHPOCBC*

The molar heat capacities of MHPOCBC were measured between 350 and 450 K. The results are listed in table 2 and plotted in figure 4. The lowest temperature phase seen in this figure is the antiferroelectric SmC_A^* phase. The melting temperature of crystalline MHPOCBC observed by our preliminary DSC measurement was 350·8 K. This value is lower than the melting point, 353·4 K, obtained by the relaxation calorimetry [12]. However, this fact does not imply that the purity of the present specimen is low. The temperature recorded here is thought to be the melting temperature of a metastable crystalline MHPOCBC because annealing just below the melting temperature was not carried out before our DSC measurement. The specimen once melted is easily supercooled below the melting point and brings about a transition to the metastable smectic I_A^* phase. The increasing heat capacities with decreasing temperature below 350 K just correspond to the high temperature tail of the phase transition between the SmC_A^* and metastable SmI_A^* phases. A small but first order phase transition from the SmC_A^* to SmC_α^* phase was detected at 373·18 K, followed by a second order phase transition to the paraelectric SmA phase at 378·42 K. These two phase transitions are shown enlarged in figure 5. As shown in figure 4, the SmA phase is transformed to the isotropic liquid at 420·49 K.

As in the case of MHPOBC, the normal heat capacity curves for the respective phase transitions were determined. For the transition from the SmC_A^* to SmA phase, the normal heat capacity curve was approximated by a third order polynomial of temperature and an additional term $(T - T_C)^{-2}$, where T_C (=344·6 K) is the transition temperature from the SmI_A^* to the SmC_A^* phase determined by our DSC measurements. The C_p data used for the least square fitting were nine C_p data in the 356–369 K range in the SmC_A^* phase and eight C_p data in the 383–395 K range in the SmA phase.

To separate the first order component inherent in the phase transition between the SmC_A^* and SmC_α^* phase, a low temperature tail of the second order transition between the SmC_α^* and SmA phases was assumed. A third order polynomial of temperature was adopted for two C_p data in the SmC_A^* phase and three C_p data in the SmC_α^* phase. The resultant curve is shown in figure 5 by the dotted line.

For the normal heat capacities concerning the transition from the SmA phase to the isotropic liquid, two straight lines were assumed. The straight line for the SmA phase was determined by use of nine C_p points in the 395–409 K range, while the line in isotropic liquid was estimated by the use of four C_p data in the range from 443 to 450 K. As shown in figure 4 by the dashed lines, these two straight lines are vertically connected at the clearing point.

For both MHPOBC and MHPOCBC, the difference between the observed and the normal heat capacities corresponds to the excess heat capacity ΔC_p due to the phase transitions. The enthalpies ($\Delta_{trs}H$) and entropies ($\Delta_{trs}S$) gained at the intersmectic and the smectic-to-isotropic transitions were determined by integration of ΔC_p with respect to T and $\ln T$, respectively. The $\Delta_{trs}H$ and $\Delta_{trs}S$ values thus obtained are listed in table 3. It should be remarked here that the SmC_α^*–SmA transition enthalpies and entropies of both compounds could possibly be underestimated. In other words, the normal heat capacities of the SmC_α^*–SmA transition would be overestimated because a straight line has simply been assumed for MHPOBC while the contribution from the high temperature tail of the SmI_A^*–SmC_A^* transition of MHPOCBC has not been sufficiently estimated.

3.3. *Phase transitions*

As described above, the present adiabatic calorimetry for MHPOBC revealed five phase transitions at 392·84, 393·74, 395·29, 396·51 and 421·73 K. These phase transitions just coincide with the phase sequence elucidated by dielectric measurements [1–3], i.e. SmC_A^*(antiferroelectric)–SmC_γ^*(ferrielectric)–SmC* (ferroelectric)–SmC_α^*–SmA(paraelectric)–I(isotropic liquid). Although the first three phase transitions are very small, they can be regarded as being first order for the following three reasons: (1) the alternating current

Table 2. Molar heat capacities of MHPOCBC.

T/K	C_p/J K^{-1} mol^{-1}	T/K	C_p/J K^{-1} mol^{-1}	T/K	C_p/J K^{-1} mol^{-1}
			Series 1		
357·432	1189·8	362·341	1187·9	367·246	1192·0
359·068	1187·8	363·977	1188·0	368·879	1193·2
360·704	1188·2	365·612	1190·7	370·510	1196·5
			Series 2		
369·593	1193·9	372·781	1201·7	376·980	1213·7
370·188	1197·0	373·103	1228·0	377·946	1222·0
370·873	1195·8	373·423	1207·4	378·911	1214·4
371·405	1196·9	374·071	1204·0	379·880	1209·3
371·891	1198·3	375·042	1207·1	380·847	1210·0
372·377	1201·1	376·012	1211·1	381·815	1210·2
			Series 3		
370·509	1196·3	373·739	1204·7	380·357	1209·0
371·114	1197·9	374·548	1205·9	381·326	1209·7
371·638	1197·9	375·518	1207·8	382·294	1211·8
372·123	1199·3	376·488	1213·3	383·262	1213·0
372·570	1200·8	377·455	1218·0	348·230	1214·6
372·936	1207·0	378·421	1223·2		
373·256	1228·0	379·388	1209·9		
			Series 4		
350·049	1231·2	354·919	1193·9	359·822	1187·2
351·664	1211·8	356·552	1190·3		
353·289	1200·7	358·186	1188·3		
			Series 5		
384·666	1213·7	402·313	1250·9	419·604	1687·9
386·279	1216·5	403·907	1256·0	420·363	8288·5
387·892	1218·8	405·502	1259·7	420·487	25256
389·502	1223·4	407·096	1263·2	420·724	6131·5
391·110	1225·0	408·688	1266·2	421·400	1361·1
392·716	1228·9	410·277	1273·1	422·656	1335·4
394·321	1232·0	411·857	1278·9	424·195	1325·5
395·923	1236·1	413·434	1285·5	425·741	1318·5
397·523	1239·4	415·008	1291·9	427·289	1313·3
399·122	1242·9	416·576	1302·0		
400·718	1247·8	418·138	1310·4		
			Series 6		
424·675	1324·2	435·033	1297·6	445·433	1296·2
426·738	1314·5	437·112	1296·6	447·512	1294·4
428·806	1308·2	439·192	1295·6	449·591	1295·2
430·879	1303·7	441·273	1295·1		
432·955	1301·2	443·353	1294·3		

(a.c.) calorimetry [7, 12] showed only a λ-type anomaly at 396 K, characteristic of a second or higher order phase transition, and failed to detect the three phase transitions which would occur between the subphases of the smectic C* phase. This fact supports that these transitions might be first order because a.c. calorimetry cannot sense the latent heat during a first order phase transition. (2) The relaxation calorimetry [12] exhibited three C_p anomalies caused by absorption of the latent heat at 392·4, 393·0 and 394·6 K, as well as the C_p peak

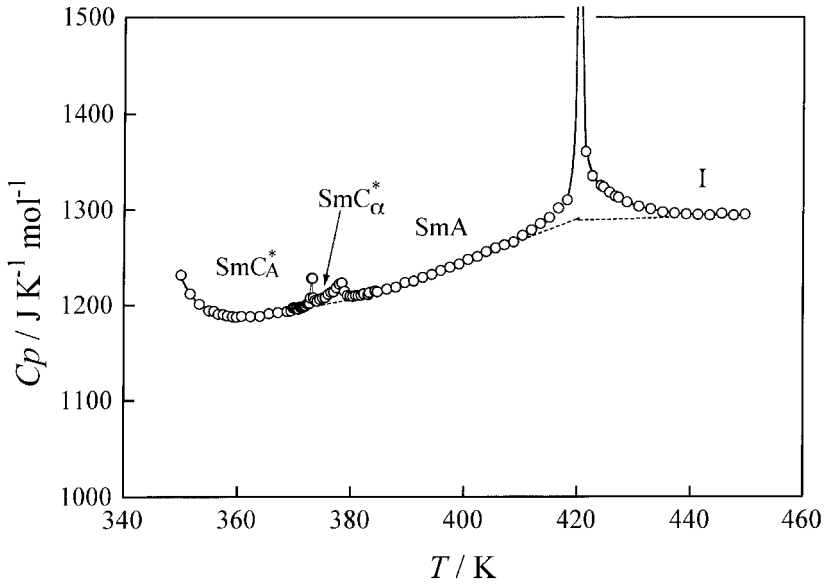

Figure 4. Molar heat capacity of MHPOCBC in the range from 350 to 450 K. Broken lines indicate the normal heat capacities.

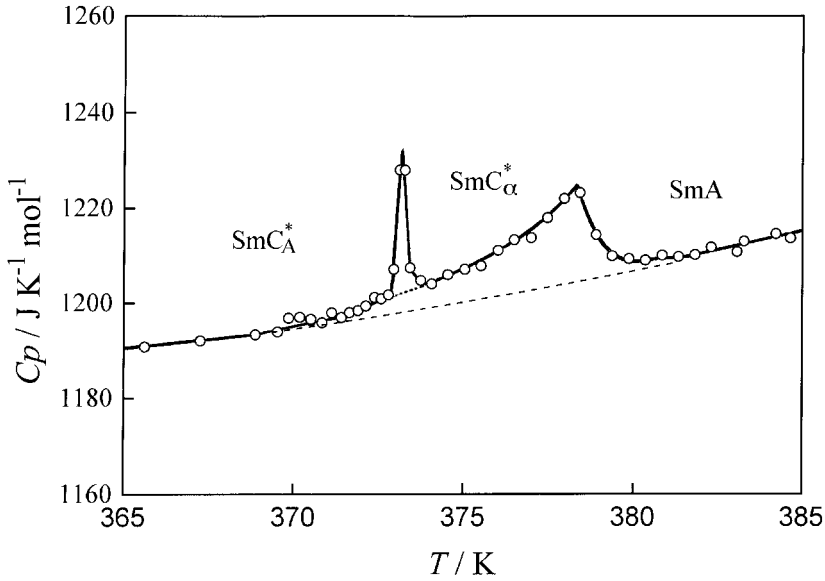

Figure 5. Molar heat capacity of MHPOCBC in the phase transition region from the SmC_A^* phase to the SmA phase. The broken line indicates the normal heat capacity, while the dotted line shows the borderline to separate the first order component of the phase transition between the SmC_A^* and SmC_α^* phases.

at 395·9 K on heating measurements that is the same anomaly as sensed by the a.c. calorimetry. It should be remarked here that these temperatures at which the relaxation calorimetry showed C_p anomalies agree well with the phase transition temperatures determined by the present adiabatic calorimetry. (3) For these three anomalies, the relaxation calorimetry revealed the existence of a thermal hysteresis characteristic of a first order phase transition.

As shown in figure 3, we assumed two kinds of normal heat capacities in order to evaluate the excess quantities associated with the three first order phase transitions: one is the normal heat capacity which separates the excess heat capacities due to all the phase transitions from the observed values, while the other is the borderline which separates the first and the second order phase transitions. As the result, the three first order phase transitions seem as if they happened additively in the course of the second order SmC_A^*–SmA phase transition. Although the existence of two baselines at a given temperature seems to be unusual, we dared to adopt this treatment to estimate separately the contributions

Table 3. Thermodynamic quantities associated with the phase transitions in MHPOBC and MHPOCBC. The enthalpy and entropy gained at the transitions ($SmC_A^* \rightarrow SmC_\gamma^*$, $SmC_\gamma^* \rightarrow SmC^*$ and $SmC^* \rightarrow SmC_\alpha^*$ for MHPOBC and $SmC_A^* \rightarrow SmC_\alpha^*$ for MHPOCBC) correspond to their first order components.

	T_{trs}/K	$\Delta_{trs}H$/J mol^{-1}	$\Delta_{trs}S$/J K^{-1} mol^{-1}
		MHPOBC	
$SmC_A^* \rightarrow SmC_\gamma^*$	392·84	16·4	0·042
$SmC_\gamma^* \rightarrow SmC^*$	393·74	18·8	0·048
$SmC^* \rightarrow SmC_\alpha^*$	395·29	14·6	0·037
$SmC_\alpha^* \rightarrow SmA$	396·51	288	0·733
$SmA \rightarrow$ Isotropic liquid	421·73	6420	15·2
		MHPOCBC	
$SmC_A^* \rightarrow SmC_\alpha^*$	373·18	11·6	0·031
$SmC_\alpha^* \rightarrow SmA$	378·42	70·3	0·187
$SmA \rightarrow$ Isotropic liquid	420·49	6280	14·9

from the first and the second order components for the following reasons. Firstly, the a.c. calorimetry detected a single C_p anomaly arising from the second order SmC_A^*–SmA transition, whose shape bears a close resemblance to the hypothetical C_p anomaly formed by truncating the three first order C_p peaks observed in the relaxation and the adiabatic calorimetries. Secondly, a second order character inherent in the phase transitions from SmC to SmA has been reported for both achiral smectogens [23, 24] and chiral smectogen [25]. Consequently, the C_p anomalies characteristic of the second order transition observed in MHPOBC and MHPOCBC can be regarded as arising from the change in the molecular tilt angle to the layer normal. On the other hand, the change in relative molecular alignments between smectic layers might give rise to a first order component in the phase transition, bringing about a small but sharp C_p peak. In what follows, therefore, we shall define the enthalpy and entropy of the SmC_A^*–SmC_γ^*, SmC_γ^*–SmC*, and SmC*–SmC_α^* transitions as the excess quantities due to the first order nature, while those of the SmC_α^*–SmA transition are attributed to the contribution from the second order component.

The transition enthalpies $\Delta_{trs}H$ thus determined for these transitions are listed in table 3. Although the relaxation calorimetry and DSC studies are semi-quantitative experimental methods compared with the adiabatic calorimetry, Ema *et al.* [12], have reported comparable $\Delta_{trs}H$ values with those determined by the present adiabatic calorimetry for the SmC_A^*–SmC_γ^*, SmC_γ^*–SmC*, SmC*–SmC_α^* and SmC_α^*–SmA transition as follows: (adiabatic = 16·4 J mol^{-1}; relaxation = 9 J mol^{-1}; DSC = 4 J mol^{-1}), (18·8; 16; 20), (14·6; 12; 9) and (288; 370; 165), respectively. The transition enthalpy observed for the second order SmC_α^*–SmA transition lies within the range characteristic of typical SmC–SmA transitions [26].

The transition entropies $\Delta_{trs}S$ for the corresponding phase transitions are 0·042, 0·048, 0·037 and 0·733 J K^{-1} mol^{-1}, respectively. At any rate, the phase transitions occurring in the SmC* subphases are extremely small from energetic and entropic viewpoints. According to the dielectric and electro-optic measurements of MHPOBC [1], molecular arrangements in the SmC* subphases are discriminated only by an interlayer relationship since the orientational ordering of molecules within each smectic layer remains essentially unchanged. This characteristic feature inherent in the SmC* subphases might be responsible for the reason why the successive phase transitions are characterized by a small transition entropy, and also why we need the borderlines to separate the excess heat capacity into the first and second order components.

On the other hand, MHPOCBC exhibited only three phase transitions at 373·18 K (SmC_A^*–SmC_α^*), 378·42 K (SmC_α^*–SmA) and 420·49 K (SmA–I). As in the case of MHPOBC, we assumed two normal heat capacity curves for the SmC_A^*–SmC_α^* transition. The transition enthalpies $\Delta_{trs}H$ for the SmC_A^*–SmC_α^* and SmC_α^*–SmA transitions are 11·6 and 70·3 J mol^{-1}, while the entropy gains $\Delta_{trs}S$ are 0·031 and 0·187 J K^{-1} mol^{-1}, respectively. The present $\Delta_{trs}H$ for the two phase transitions are comparable with 12 and 60 J mol^{-1} obtained from DSC measurements [10] and 65 J mol^{-1} for the SmC_α^*–SmA transition obtained by a.c. calorimetry [12]. As in the case of MHPOBC, the enthalpy gained at the second order SmC_α^*–SmA transition of MHPOCBC is also in the range of typical SmC–SmA transitions [26].

Although MHPOCBC has essentially the same molecular structure as MHPOBC (see figure 1), the

antiferroelectric SmC_A^* phase is directly transformed to the fancy SmC_α^* by skipping the ferrielectric SmC_γ^* and ferroelectric SmC* phases. This fact is confirmed by the present adiabatic calorimetry. Moreover, the cumulative transition entropy, 0·218 J K^{-1} mol^{-1}, from the antiferroelectric SmC_A^* to the paraelectric SmA phase is much smaller than 0·860 J K^{-1} mol^{-1} found for MHPOBC. Interestingly, however, the $\Delta_{trs}S$ values of the SmA–I transition for MHPOBC and MHPOCBC are 15·2 and 14·9 J K^{-1} mol^{-1}, essentially the same values. The enthalpy values of the SmA–I transition for MHPOBC and MHPOCBC are 6·48 and 6·28 kJ mol^{-1}, respectively, and are in the range of an ordinary SmA–I transition [26].

3.4. *Phase behaviour and Devil's staircase*

The present antiferroelectric liquid crystals exhibit one or more subphases between SmC_A^* and SmA, i.e. SmC_γ^*, SmC* and SmC_α^* for MHPOBC, and SmC_α^* for MHPOCBC. In these subphases, the molecules are thought to lie on layers and tilt to the layer normal. This type of layer structure is typical for the SmC phase and is also encountered in the antiferroelectric SmC_A^* phase. However, the long range orientational structure of the molecular dipole moments is different among these phases. Except for a slight precession of a few degrees per layer caused by chirality, the dipole moments in adjacent layers are parallel in the ferroelectric SmC* phase, while antiparallel in the antiferroelectric SmC_A^* phase. In the ferrielectric SmC_γ^* phase the relative orientation of the dipole moments between adjacent layers (parallel or antiparallel) changes regularly along the layer normal.

Fukuda *et al.* [1] adopted the one-dimensional Ising model to explain the change in the direction of the dipole moments along the smectic layers with temperature. The ratio $q_T = n/m$, eventually reflecting a fraction of ferroelectric ordering, was introduced to systematically classify ferro-, ferri- and antiferroelectric smectic phases, where m denotes the number of layer boundaries involved in one cycle of the orientational period of the dipole moments and n stands for the number of the boundaries across which two adjacent dipole moments are parallel (i.e. ferroelectric) in the m layer boundaries. Consequently, $q_T = 1$ corresponds to the ferroelectric SmC* phase, and $q_T = 0$ for the antiferroelectric SmC_A^* phase. As described in § 3.1, the ferrielectric SmC_γ^* phase of MHPOBC is composed of ferroelectric and antiferroelectric structures in the ratio of 1 : 2. Therefore, q_T for the SmC_γ^* phase corresponds to 1/3. This feature in the SmC_γ^* phase can be described by the one-dimensional Ising model. This model can predict the spontaneous polarization and the apparent tilt angle as a function of q_T. The q_T value is governed by the pairing energy of the dipole moments and the molecular packing entropy. Many orientational structures of the dipole moments are possible between $q_T = 0$ and 1. This feature is characteristic of the one-dimensional Ising model and called the 'Devil's staircase'. Among the staircases, the spontaneous polarization and the apparent tilt angle take maximum values when $q_T = 1/3$. The q_T value, derived from the model, agrees with the experimental value observed for the ferrielectric SmC_γ^* phase of MHPOBC. The ferrielectric structure seems to be energetically stabilized at $q_T = 1/3$ as exemplified by the SmC_γ^* phase of MHPOBC.

The one-dimensional Ising model also alludes to the existence of stable ferrielectric phases other than the SmC_γ^* phase. Especially, Bak and Bruinsma [21] derived theoretically that the ferrielectric phase with $q_T = 1/2$ or 1/4 is likewise stable as that with $q_T = 1/3$. In fact the ferrielectric phase with $q_T = 1/2$ has been observed by miscibility tests of two antiferroelectric liquid crystals [27]. However, neither MHPOBC nor MHPOCBC exhibits any ferrielectric phases other than $q_T = 1/3$. The polymorph of the ferrielectric SmC phase is attributed to the balance between the strength of the antiferroelectricity and the strength of the ferroelectricity of the mesogen [1]. The number of the ferrielectric phase is thought to increase when these two strengths become comparable. In this sense, both MHPOBC and MHPOCBC studied here are far from the balance between these two factors, which prevents the appearance of plural ferrielectric phases.

The SmC_α^* phase has a complicated structure of layers and molecular dipole moments in comparison to the other smectic C phases. An important feature of the SmC_α^* phase is the considerably reduced ability in forming the structures of ferro- and antiferroelectric smectic C phases. This leads to the thermally excited C-director disclinations, and the correlation length of the molecular ordering is greatly shortened in the SmC_α^* phase compared to the SmC_A^* phase. In spite of this feature, electro-optic measurements clarified that the SmC_α^* phase possesses the antiferroelectric structure in the high temperature region, and the ferrielectric structure in the low temperature region [28]. This means that the orientational structure of the dipole moments changes successively with temperature. As a result, the SmC_α^* phase exhibits another Devil's staircase which is different from the Devil's staircase encountered in the change from the SmC_A^* to the SmC* phase. As the phase sequence is ferroelectric SmC*–ferrielectric SmC_γ^*–antiferroelectric SmC_A^* on cooling, it seems somewhat curious that the ferroelectricity increases with decreasing temperature within the SmC_α^* phase. The change in the molecular tilt angle is thought to be responsible for this behaviour [1]. An increase in the tilt angle would

enhance an excluded volume favourable to the formation of the ferroelectric structure.

Since the Devil's staircase phase structure is applicable to the SmC^*_α phase, it is anticipated that a certain ferrielectric phase similar to the SmC^*_γ phase might appear as a subphase of the SmC^*_α phase. However, no ferrielectric phase was observed as an independent phase in the SmC^*_α region for either MHPOBC or MHPOCBC. The heat capacity is continuously changing within experimental errors and any peaks or heat capacity anomalies suggesting the existence of new phases were not detected in the SmC^*_α region (see figures 3 and 5). For the appearance of a ferrielectric phase, competition between ferroelectricity and antiferroelectricity plays an important role. As these forces are greatly reduced in the SmC^*_α phase in comparison to the case of the SmC^*_γ phase of MHPOBC, the orientational structure of the dipole moments seems to change continuously without any phase transitions.

References

[1] Fukuda, A., Takanishi, Y., Isozaki, T., Ishikawa, K., and Takezoe, H., 1994, *J. mater. Chem.*, **4,** 997.

[2] Hiraoka, K., Ouchi, Y., Takezoe, H., Fukuda, A., Inui, S., Kawano, S., Saito, M., Iwane, H., and Itoh, K., 1991, *Mol. Cryst. liq. Cryst.*, **199,** 197.

[3] Hiraoka, K., Takezoe, H., and Fukuda, A., 1993, *Ferroelectrics*, **147,** 13.

[4] Takezoe, H., Lee, J., Chandani, A., Gorecka, E., Ouchi, Y., and Fukuda, A., 1990, *Ferroelectrics*, **113,** 187.

[5] Li, J., Takezoe, H., Fukuda, A., and Watanabe, J., 1995, *Liq. Cryst.*, **18,** 239.

[6] Takanishi, Y., Takezoe, H., Fukuda, A., Komura, H., and Watanabe, J., 1992, *J. mater. Chem.*, **2,** 71.

[7] Chandani, A., Ouchi, Y., Takezoe, H., Fukuda, A., Terashima, K., Furukawa, K., and Kishi, A., 1989, *Jap. J. appl. Phys.*, **28,** L1261.

[8] Hori, K., Kawahara, S., and Ito, K., 1993, *Ferroelectrics*, **147,** 91.

[9] Kim, K., Takanishi, Y., Ishikawa, K., Takezoe, H., and Fukuda, A., 1994, *Liq. Cryst.*, **16,** 185.

[10] Miyachi, K., Matsushima, J., Takanishi, Y., Ishikawa, K., Takezoe, H., and Fukuda, A., 1995, *Phys. Rev. E*, **52,** R2153.

[11] Jin, B., Ling, Z., Takanishi, Y., Ishikawa, K., Takezoe, H., Fukuda, A., Kakimoto, M., and Kitazume, T., 1996, *Phys. Rev. E*, **53,** R4295.

[12] Ema, K., Yao, H., Kawamura, I., Chan, T., and Garland, C., 1993, *Phys. Rev. E*, **47,** 1203.

[13] Ema, K., Watanabe, J., Takagi, A., and Yao, H., 1995, *Phys. Rev. E*, **52,** 1216.

[14] Ema, K., Takagi, A., and Yao, H., 1996, *Phys. Rev. E*, **53,** R3036.

[15] Ema, K., Ozawa, M., Takagi, A., and Yao, H., 1996, *Phys. Rev. E*, **54,** R25.

[16] Isozaki, T., Suzuki, Y., Kawamura, I., Mori, K., Yamamoto, N., Yamada, Y., Orihara, H., and Ishibashi, Y., 1991, *Jap. J. appl. Phys.*, **30,** L1573.

[17] Ema, K., Yao, H., Fukuda, A., Takanishi, Y., and Takezoe, H., 1996, *Phys. Rev. E*, **54,** 4450.

[18] Sorai, M., Kaji, K., and Kaneko, Y., 1992, *J. chem. Thermodyn.*, **24,** 167.

[19] Laux, V., Isaert, N., Nguyen, H., Cluzeau, P., and Destrade, C., 1996, *Ferroelectrics*, **179,** 25.

[20] Hiraoka, K., Takanishi, Y., Skarp, K., Takezoe, H., and Fukuda, A., 1991, *Jap. J. apply. Phys.*, **30,** L1819.

[21] Bak, P., and Bruinsma, R., 1982, *Phys. Rev. Lett.*, **49,** 249.

[22] Bak, P., 1986, *Phys. Today*, **39,** 38.

[23] Huang, C., and Viner, J., 1982, *Phys. Rev. A*, **25,** 3385.

[24] Meichle, M., and Garland, C., 1983, *Phys. Rev. A*, **27,** 2624.

[25] Lien, S., Huang, C., and Goodby, J., 1984, *Phys. Rev. A*, **29,** 1371.

[26] Marzotko, D., and Demus, D., 1975, *Pramana Suppl.*, **1,** 189.

[27] Isozaki, T., Fujikawa, T., Takezoe, H., Fukuda, A., Hagiwara, T., Suzuki, Y., and Kawamura, I., 1993, *Phys. Rev. B*, **48,** 13 439.

[28] Takanishi, Y., Hiraoka, K., Agrawal, V., Takezoe, H., Fukuda, A., and Matsushita, M., 1991, *Jap. J. appl. Phys.*, **30,** 2023.